SAND2018-7797B

Resolving Properties of Entangled Polymers Melts through Atomistic Derived Coarse-Grained Models

Gary S. Grest,[1] K. Michael Salerno,[2] Brandon L. Peters,[1] Ting Ge,[3] and Dvora Perahia[4]

[1]Sandia National Laboratories, Albuquerque, New Mexico 87185 USA

[2]U. S. Naval Research Laboratory, Washington, DC 20375, USA

[3]Department of Mechanical Engineering and Materials Science, Duke University, Durham, North Carolina 27708, USA and

[4]Department of Chemistry and Department of Physics and Astronomy, Clemson University, Clemson, South Carolina 29634, USA

Abstract

Coupled length and time scales determine the dynamic behavior of polymers and polymer nanocomposites, which underlie their unique properties. To resolve the properties over large time and length scales it is imperative to develop coarse grained models which retain atomistic specificity. Here we probe the degree of coarse graining required to access large length and time scales and simultaneously retain significant atomistic details. The degree of coarse graining in turn sets the minimum length scale instrumental in defining polymer properties and dynamics. Using polyethylene as a model system, we probe how the scale of coarse-graining affects the measured dynamics with different number of methylene groups per coarse-grained bead. Using these models, it is currently possible to simulate polyethylene melts for times of order 1 millisecond. This allows one to study a wide range of properties from chain mobility to viscoelastic response for well-entangled polymer melts while retaining atomistic detail.

I. Introduction

Polymer properties depend on a wide range of coupled length and time scales, with unique viscoelastic properties stemming from interactions down to the atomistic level. The need to probe polymers across time and length scales to capture polymer behavior makes probing dynamics, and particularly computational modeling, inherently challenging. With increasing molecular weight, polymer melts become highly entangled and the long-time diffusive regime becomes computationally inaccessible using atomistic simulations. While the largest length scales of polymer dynamics are controlled by entanglements, the shortest time and length scales required to resolve dynamic properties are not obvious. This knowledge is critical for developing models that can transpose atomistic details into the long-time scales needed to model long, entangled polymer chains.

One path to overcoming the computational challenge of large time and length scales in polymers and polymer nanocomposites is to coarse grain (CG) the polymer, reducing the number of degrees of freedom and increasing the fundamental time scale. The effectiveness of this process depends on retaining the smallest length scale essential to capturing the polymer dynamics. The process of coarse graining amounts to combining groups of atoms into pseudoatom beads and determining the bead interaction potentials. Simple models like the bead-spring model (Kremer and Grest 1990, Grest 2016) capture the main characteristics of polymers, but disregard atomistic details. These models cannot quantitatively describe properties like structure, local dynamics, or densities. Numerous recent studies have worked to bridge the divide between atomistic and coarse models, developing new approaches to drive computational studies to larger length and time scales while maintaining relevant sub-nanometer details (Müller-Plathe 2002, Peter and Kremer 2009, Fritz, Koschke et al. 2011, Li, Abberton et al. 2013). The mapping scheme which defines which atoms are combined into a pseudoatom bead are not unique and depend on the specific system and the local properties one wants to retain. For polystyrene (PS), for example, there are at least seven different mapping schemes in which each PS monomer is represented by either one or two CG beads (Karimi-Varzabeh, van der Vegt et al. 2012). For flexible polymers, such as polyethylene (Fukunaga, Takimoto et al. 2002, Padding and Briels 2002, Guerrault, Rousseau et al. 2004, Ashbaugh, Patel et al. 2005, Chen, Qian et al. 2006, Padding and Briels 2011), polybutadiene (Maurel, Schnell et al. 2012), poly(dimethylsiloxane) and polyisobutylene (Maurel, Goujon et al. 2015), multiple monomers are combined to form one CG bead. However, few of these studies have explored the effect of varying the degree of coarse-graining on the properties of polymer melts (Abrams and Kremer 2003, Harmandaris, Reith et al. 2007, Karimi-Varzabeh, van der Vegt et al. 2012, Salerno, Agrawal et al. 2016, Salerno, Agrawal et al. 2016, Dallavalle and van der Vegt 2017, Peters, Salerno et al. 2017).

Here, using linear polyethylene as a model system, we review how the degree of coarse-graining effects the macromolecular structure and dynamics (Salerno, Agrawal et al. 2016, Salerno, Agrawal et al. 2016, Peters, Salerno et al. 2017). The backbone of polyethylene (PE) consists of -CH_2– methylene groups, which are a natural coarse-graining unit. Probably the most well-known CG models for PE is the united atom (UA) model (Siepmann, Karaborni et al. 1993, Paul, Yoon et al. 1995, Martin and Siepmann 1998, Nath, Escobedo et al. 1998), which combines each CH_2/CH_3 group into one pseudoatom. The UA interaction parameters are determined phenomenologically to reproduce physical properties such as densities and critical temperatures. Going beyond the UA model, PE has previously been studied using CG models with beads of $\lambda = 3 - 48$ methylene groups per CG bead (Padding and Briels 2001, Fukunaga, Takimoto et al. 2002, Padding and Briels 2002, Guerrault, Rousseau et al. 2004, Ashbaugh, Patel et al. 2005, Chen, Qian et al. 2006, Curcó and Alemán 2007, Padding and Briels 2011). However as most of these studies used a large degree of coarse graining ($\lambda \sim 20$) to study dynamics, an extra constraint is needed to prevent chains cutting through each other (Padding and Briels 2002). Here we focus on systems with fewer methylene groups per CG bead ($2 \leq \lambda \leq 6$) where we could largely (but not completely as discussed below) avoid including extra constraints to avoid chains cutting each other.

Figure 1 illustrates how the CG models with λ = 2-6 methylene groups per CG bead represent the underlying atomistic configuration. Though the chemical structure of PE is simple, it is a thermoplastic material useful in many applications, with tunable mechanical properties determined by the degree of branching. Using these CG models, we show here that one can capture polymer chain dynamics for long entangled polymers for time scales of order 1 ms using models that accurately represent atomistic detail. Accessing these large length and time scales, which are simply not accessible using fully atomistic models,

allows one to measure a wide range of properties from the single chain dynamics to the stress relaxation function and shear viscosity which depend on a hierarchy of length and time scales.

II. Model and Methodology

Each of the CG potentials was derived from a fully atomistic molecular dynamics simulation of a melt of C_nH_{2n+2} with n=96 for λ=2, 3, 4, and 6 and n=95 for λ=5 (Salerno, Agrawal et al. 2016, Salerno, Agrawal et al. 2016, Peters, Salerno et al. 2017). The atomistic simulations used the All Atom Optimized Potentials for Liquid Simulations (OPLS-AA) potential (Jorgensen, Madura et al. 1984, Jorgensen, Maxwell et al. 1996) with modified dihedral coefficients (Siu, Pluhackova et al. 2012). These modified OPLS-AA parameters reproduce the experimental static and dynamic chain properties for long alkanes better than the original OPLS-AA parameters. Tabulated CG bond potentials $U_B(l)$ and angle potentials $U_A(\theta)$ were determined by Boltzmann inversion of the atomistic bond length and angle distributions,

$$U_b(l) = -k_B T \log[\frac{P(l)}{l^2}]$$

$$U_A(\theta) = -k_B T \log[\frac{P(\theta)}{\sin\theta}],$$

where *l* is the bond length for CG beads overlaid on the atomistic reference configurations and θ is the angle between CG bead triplets from the atomistic reference configuration. These two potentials were determined at temperature T = 400 and 500 K and found to be independent of temperature (Peters, Salerno et al. 2017). In the current study, dihedral interactions were not included. However, recently Salerno and Bernstein (Salerno and Bernstein 2018) have shown that for differences in the end-to-end distance $\langle R^2 \rangle$ of up to 40% can occur for CG models with no dihedral interaction. This error is a result of correlations inherent to the CG models that can be represented as a dihedral interaction. Including a dihedral interaction in CG models of PE can effectively correct this error in the chain stiffness.

Tabulated nonbonded potentials were calculated by a multi-step iterative Boltzmann inversion process (Müller-Plathe 2002, Reith, Pütz et al. 2003, Voth 2008). The intermolecular radial distribution function g(r) from the atomistic simulation was used as the target for iteration of the nonbonded potentials. The resulting potentials, while giving excellent agreement between the CG g(r) and the target g(r), always resulted in a pressure which was significantly larger than that of the atomistic system. A pressure correction (Milano and Müller-Plathe 2005, Sun and Faller 2005, Wang, Junghans et al. 2009) was then applied to bring the pressure of the CG and atomistic systems into agreement. This resulted in a slight increase of the pair correlation function in the vicinity of the first peak for the CG model compared to the target but this difference was found to have no effect on the chain mobility and viscoelastic response of the system (Salerno, Agrawal et al. 2016, Peters, Salerno et al. 2017). The resulting potentials for four values of λ at 500 K are shown in Figure 2. Unfortunately, these CG potentials are not necessarily transferable to other temperatures. For example, with λ = 4 the attractive well for the CG potential developed at 500 K is 20% deeper compared with that developed at 400 K (Peters, Salerno et al. 2017). Comparison of these potentials with the standard Lennard-Jones (LJ) 12:6 potential, which is often used in bead–spring models of polymers (Kremer and Grest 1990, Grest 2016), shows that these atomistically inspired CG potentials are softer with a much shallower attractive well than the LJ 12:6 potential (Peters, Salerno et al. 2017). Since PE is locally stiff, as the degree of coarse graining increases, the methyl groups

in each CG bead take up less of the volume. As a result, the nonbonded potentials become softer with increasing λ.

For large degrees of coarse graining, one must also include extra constraints so that the chains cannot cut through each other (Padding and Briels 2002). For polyethylene, even the $\lambda = 6$ model has a surprisingly large equilibrium bond distance relative to the bead diameter which allows chains to occasionally cut through each other. Therefore, in our simulations we added a modified soft segmental repulsive potential (Sirk, Slizoberg et al. 2012) CG beads to inhibit chain crossing for λ=6. Complete details of the model and methodology are given in Salerno et al. (Salerno, Agrawal et al. 2016).

One important advantage of CG models is that by eliminating the finest degrees of freedom, the time step in a molecular dynamics simulation is significantly larger than for fully atomistic models. We found that one can use a time step δt = 20 fs for λ = 4, 5 and 6 and 10 fs for λ = 3. However, for λ = 2, δt is only 4 fs, comparable to that commonly used for atomistic (1 fs) and UA (1-2 fs) models. The reduction in the number of degrees of freedom in a system also creates a smoother free-energy landscape compared with fully atomistic or UA model simulations. While strong frictional and stochastic forces can be used to slow down the dynamics of the CG model to match those of the atomistic model (Salerno, Agrawal et al. 2016), one can take advantage of this increase in the local dynamics of the CG model to simulate effectively much longer time scales (Harmandaris and Kremer 2009, Fritz, Koschke et al. 2011). While the former approach may be useful for coarse graining small molecules, for entangled polymers which already have inherently slow dynamics, this additional speed up for CG models is very advantageous. Combining the reduction in the number of atoms that one must simulate, the significant larger simulation time steps and the increase in the dynamics from the smoother free energy surface, the effective simulation time is effectively increased by at least three orders of magnitude for λ = 4-6, allowing one to reach times scales not accessible using fully atomistic simulations. Computationally for PE, λ = 4 and 5 are the most efficient since λ = 6 requires the addition of an extra bead between each CG bead to avoid chains cutting through each other. All of the simulations presented here were performed using the Large Atomic Molecular Massive Parallel Simulator (LAMMPS) molecular dynamics simulation code (Plimpton 1995), though any MD software package which allows tabulated forces for bond, angle and non-bonded potentials could be used.

III. Results

In Salerno et al. (Salerno, Agrawal et al. 2016, Salerno, Agrawal et al. 2016), we probed the dynamics of polymers as the number of atoms included in a CG bead is varied from λ = 2 to 6. We found that independent of the degree of coarse graining, the static and dynamic properties are similar once the dynamic scaling factor α and non-crossing constraint for λ = 6 are included. Using these CG models, we have been able to reach times of order 1 ms, allowing us to measure several quantities which can be compared directly to experiments, including the stress relaxation function, plateau modulus and shear viscosity. Here, some examples of our results are presented to illustrate the power of the coarse graining methodology to sample times and length scales not accessible by atomistic simulations while retaining chemical specificity.

Coarse graining reduces the number of degrees of freedom in a system, creating a smoother free-energy landscape compared with fully atomistic simulations (Harmandaris and Kremer 2009, Fritz, Koschke et al.

2011). This can be seen by measuring the mean squared displacement (MSD) for the atomistic model of PE with n = 96 and 480 carbons to the equivalent CG model as shown in Figure 3(a). The mobility of the chains in the CG models is clearly larger than in atomistic simulations. By scaling the time for each of the CG models the results fall on a single collapsed curve for each chain length for the atomistic and CG models as shown in Figure 3(b). Notably, a single scaling factor α is required for each λ, independent of chain length. For T = 500K, α varied from 6-9 for λ = 2-6 and increases with decreasing temperature (Peters, Salerno et al. 2017). For λ = 4, α = 6.2 for T = 500K and increases to ~12 at 400 K. Combining the effects of fewer interaction sites, a larger time step and the dynamic scaling factor α, these CG models allows one to study well entangled chains for long times.

Results for the MSD of the center of mass $g_3(t) = \langle(\mathbf{r}_{\mathrm{cm}}(t) - \mathbf{r}_{\mathrm{cm}}(0))^2\rangle$ and motion of the center 4 beads $g_1(t) = \langle(\mathbf{r}_{\mathrm{i}}(t) - \mathbf{r}_{\mathrm{i}}(0))^2\rangle$ for chain lengths n = 1920, 2560 and 4000 for λ = 4 at 500 K are shown in Figure 4. The experimental entanglement length for PE is 1.1-1.2 kg/mol or n ~80 (Fetters, Lohse et al. 1999, Vega, Rastogi et al. 2004). For n = 1920 and 2560, the MSD has reached the diffusive regime where MSD $\sim t^1$. Over intermediate time scales for all 3 systems, the chains show the expected $t^{1/4}$ scaling predicted the tube model (de Gennes 1971, Doi and Edwards 1986). The diffusion constant $D = g_3(t)/6t$ for $t > \tau_d$ is shown in Figure 5 as a function of n. For large n, D follows a power law decay $D = D_1 n^{-2.18}$ where D_1 = 3.08 x 10^{-6} m^2/s. The decay of D with a power law greater than 2 for large M is consistent with experimental results (Lodge 1999).

From the crossover time t_e^* from the early time $t^{1/2}$ Rouse regime to $t^{1/4}$ reptation, one can extract the tube diameter d_T and the entanglement time τ_e. Assuming the distribution of segment displacement along the tube is Gaussian on the scale of the tube diameter d_T, then the entanglement time $\tau_e = \frac{9}{\pi} t_e^*$ (Hou 2017). From Figure 4, this crossover time is $t_e^* \sim 14$ ns, which give τ_e ~ 40 ns. Note that in the literature τ_e and t_e^* are assumed to be the same. The MSD of the center monomers at t_e^*, $g_{1e}^* = \frac{2}{3\pi} d_T^2$ gives a tube d_T ~ 4.9 nm (Hou 2017). If one neglects $the\ \frac{2}{3\pi}$ prefactor between g_{1e}^* and d_T^2, which is often done in the literature (Hsu and Kremer 2016), then d_T ~ 2.3 nm. The later value is in good agreement with the assumption that $d_T^2 = 2\, R_g^2\,(N_e)$, which gives d_T ~ 2.2 nm. Neutron spin-echo experiments by Richter et al. (Richter, Butera et al. 1992) and Schleger et al. (Schleger, Farago et al. 1998) estimate τ_e ~ 5 ns and tube diameter $d = \sqrt{3} d_T \cong 4.35$ nm or $d_T \sim 2.5$ nm (Hsu and Kremer 2017). Thus the crossover times and distances of the CG model capture the essential aspect of the polymer motion, demonstrating that one can capture long time and length scales with CG models while accounting for atomistic detail.

The stress response function after a small perturbation G(t) is one of the most important experimental measurements for polymers. For long entangled polymers, at short times G(t) decays as the chains locally relax in response to the perturbation like any fluid. However, for intermediate times G(t) plateaus at $G_N^o = \frac{4}{5}\rho RT/M_e$ where M_e is the entanglement molecular weight. This plateau region in G(t) occurs for intermediate times where the chains are assumed to move in a tube due to entanglements from the other chains. Only after the chains have reached the diffusive regime, does G(t) relax to zero. The relaxation modulus for each of our CG models was measured for different chain lengths via equilibrium stress autocorrelations. Figure 6 shows G(t) for n = 1920 and 4000 for λ = 4, where time has been scaled by the dynamic rescaling factor α. The solid lines in Figure 4 are a fit to the Likhtman-McLeish (LM) expression (Likhtman and McLeish 2002)

$$G(t) = \frac{k_B T}{nv}\left[\frac{1}{5}\sum_{p=1}^{Z}\left(4\mu(t)R(t) + e^{-tp^2/\tau_R}\right) + \sum_{p=Z+1}^{N} e^{-2tp^2/\tau_R}\right]$$

where

$$\mu(t) = \frac{8}{\pi^2}\sum_{q=1,odd}^{\infty}\frac{1}{q^2}\exp\left(-\frac{q^2 t}{\tau_d}\right)$$

is the Doi-Edwards reptation stress relaxation function (Doi and Edwards 1986) with terminal relaxation time τ_d and the double-reptation expression for constraint release $R(t) = \mu(t)$ is assumed (Marrucci 1985). The key quantity in this expression is the single-chain memory function $\mu(t)$ for the fraction of the primitive chain which has not escaped from its original tube after a time t. The fitting parameters are the number of entanglements per chain Z, the terminal relaxation time τ_d, and the Rouse time τ_R. The volume of a CH_2 monomer is $v = 0.031nm^3$ for $\rho = 0.76\,\mathrm{g/cm^3}$. The best-fit results are $Z = 23 \pm 1$, $\tau_d = (1.49 \pm 0.04) \times 10^5$ ns, $\tau_R = (2.60 \pm 0.16) \times 10^4$ ns for $n = 1920$, and $Z = 40 \pm 1$, $\tau_d = (5.55 \pm 0.09) \times 10^5$ ns, $\tau_R = (8.18 \pm 0.32) \times 10^4$ ns for $n = 2560$. Based on these results, the plateau modulus $G_e = 4Zk_BT/5nv = 2.3$ MPa for $n = 1920$ and 1.8 MPa for $n = 4000$, the entanglement time $\tau_e = \tau_R/Z^2 = 49.1\,ns$ for $n = 1920$ and $51.1\,ns$ for $n = 4000$, consistent with the entanglement times extracted above from the MSD. The entanglement molecular weight $M_e = n/Z \times 14\,\mathrm{g/mol} = 1.2\,\mathrm{kg/mol}$ for $n = 1920$ and $1.4\,\mathrm{kg/mol}$ for $n = 4000$, which is consistent with experimental results for M_e (Fetters, Lohse et al. 1999, Vega, Rastogi et al. 2004). For comparison, the longest chain systems we could study using fully atomistic simulations is n = 480, which is not long enough and cannot be simulated for long enough to observe a plateau in G(t).

Polymer entanglements can be directly determined by the primitive path analysis (PPA) algorithm first developed by Everaers et al. (Everaers, Sukumaran et al. 2004) In the PPA, the chain ends are fixed and the intrachain excluded volume interactions are turned off, while retaining the interchain excluded volume interactions. The energy of the system is then minimized by slowly cooling the system to T = 0. The entanglement molecular weight M_e can then be obtained from the average contour length of the primitive path and the end-to-end distance of the chain (Everaers, Sukumaran et al. 2004). In the standard PPA method (Everaers, Sukumaran et al. 2004), the chains maintain the same diameter during the length minimization process. Alternatively one can introduce extra beads to reach the limit of zero thickness chains (Hoy and Grest 2007). These two methods are often referred to as thick and thin chain PPA respectively. Although both methods can give good estimates of the entanglement length in a polymer melt, the effect of the bead size or CG level λ should be considered. In this context, it is important to be able to represent a single reference configuration with various λ and calculate the same primitive path length, independent of λ. We found that the thick-chain PPA method produces results that vary by 15-20% with λ. Hence, we adopt a procedure that is more like the thin-chain PPA method to reliably reproduce the primitive path length and entanglement length, independent of the coarse graining level λ.

The primitive path contour length and the resulting entanglement length were estimated by inserting four (or nine) beads between each bead for λ = 4, setting the bead diameters to 1.3 Å (0.65 Å) and reducing the backbone bond length at constant tension. The primitive path contour length was computed for n = 480 for 10 independent melt configurations. The primitive path length was estimated to be 19.8 nm,

with lower and upper estimates of 24 and 31 CG beads for the entanglement length, based on the estimator proposed by Hoy et al. (Hoy, Foteinopoulou et al. 2009). These thin chain PPA values correspond to entanglement mass M_e = 1.34 and 1.74 kg/mol, somewhat higher than the estimate from based on the plateau modulus.

Using non-equilibrium molecular dynamics simulations, we measured the shear viscosity η as a function of shear rate over a wide range of shear rates from the shear independent regime at low shear rates to the shear thinning regime at high shear rates. Results for η versus scaled shear rate for n=96 to 1920 are presented in Salerno et al. (Salerno, Agrawal et al. 2016). Our results for the zero shear rate viscosity η showed a crossover from a n^1 power law for small n to $n^{3.4}$ for large n at $n_c \sim 250$ or molecular weight ~ 35 kg/mol in excellent agreement with the experiment (Ferry 1980, Graessley and Edwards 1981).

While most studies of polymer melts model a homopolymer in which all the chains have the same length or at most a binary mixture of two lengths, experimental systems are never uniform. They are highly dispersed with a range of chain lengths. The standard way to characterize molar-mass dispersity is the dispersity index $Đ_M$ defined by $Đ_M = M_w/M_n$, where M_w is the weight average molecular weight and M_n is the number average molecular weight. M_n is more sensitive to molecules of low molecular mass, while M_w is more sensitive to molecules of high molecular mass. The best case experimentally for long polymers is $Đ_M$ ~1.02 but in some cases $Đ_M$ >2. Even for $Đ_M$ ~ 1.02, the ratio of the largest to shortest chain is larger than 2. How dispersity effects the chain mobility and viscoelastic response is difficult to predict theoretically and makes testing theoretical models, which makes testing theoretical models challenging due to the assumption that the system contain only uniform polymers.

Using our coarse grained model with λ = 4, we (Peters, Salerno et al. 2018) have recently initiated a study of the effect of polydispersity on polymer chain mobility and viscoelastic properties. We built dispersed systems of 2000 chains for $Đ_M$ = 1.02, 1.04 and 1.08 and 4000 chains for $Đ_M$ = 1.16 for highly entangled chains of molecular weight M_w = 36 kg/mol (n=2650 CH_2 monomers or 640 CG beads). This chain length was chosen since it is long enough for the chains to be well entangled but short enough that the system fully relaxes on the time scales accessible to simulations (~600-800 μs). For short times, the monomers in the center of the chain diffuse the same independent of the degree of dispersity. However, for longer times the MSD of the more dispersed samples move faster. Unlike experiment, simulations can be used to extract more detailed information of how the various chain populations diffuse. For example, the average diffusion constant of all the chains as well as the shortest and longest can be readily determined as shown in Figure 7. As $Đ_M$ increases the spread in the diffusion constant increases very rapidly with $Đ_M$ while the average value of D increases by only a factor of 50% over this range.

IV. Conclusions

Here we probed the structure and dynamics of polymers with various numbers of atoms included in a coarse-grained bead. We have shown that for long, entangled polymers, independent of the degree of coarse graining, all static and dynamic properties are essentially the same once the dynamic scaling factor α and non-crossing constraint for λ=6 are included. Due to the larger time step and reduced number of degrees of freedom of the coarse-grained model as well as the smoother free energy surface, the coarse-grained simulations are effectively 3-4 orders of magnitude faster than the fully atomistic model, depending on the degree of coarse graining and the temperature. Of the five models studied, λ = 4 and 5

offer the optimum performance since larger degrees of coarse graining require an additional non-crossing constraint which negates the gain in effective speed due free pairwise interactions. This translates to simulation times of hundreds to thousands of μs, which allows us to measure many quantities which can be compared directly to experiments, including the stress relaxation function, plateau modulus and shear viscosity. With this speedup, one can readily extend the present study to longer chains as well as including short and long chain branching in addition to the study of polydispersed systems.

ACKNOWLEDGMENTS

KMS was supported in part by the National Research Council Associateship Program at the U.S. Naval Research Laboratory. DP kindly acknowledged NSF DMR1611136 for partial support. This work was supported by the Sandia Laboratory Directed Research and Development Program. Research was carried out in part at the Center for Integrated Nanotechnologies, a U.S. Department of Energy, Office of Basic Energy Sciences user facility. Sandia National Laboratories is a multimission laboratory managed and operated by National Technology and Engineering Solutions of Sandia, LLC, a wholly owned subsidiary of Honeywell International, Inc., for the U.S. Department of Energy's National Nuclear Security Administration under Contract DE-NA-0003525.

Abrams, C. F. and K. Kremer (2003). "Combined Coarse-Grained and Atomistic Simulation of Liquid Bisphenol A–Polycarbonate: Liquid Packing and Intramolecular Structure." Macromolecules **36**: 260–267.

Ashbaugh, H. S., H. A. Patel, S. K. Kumar and S. Garde (2005). "Mesoscale model of polymer melt structure: Self-consistent mapping of molecular correlations to coarse-grained potentials." J. Chem. Phys. **122**: 104908.

Chen, L.-J., H.-J. Qian, Z.-Y. Lu, Z.-S. Li and C.-C. Sun (2006). "An automatic coarse-graining and fine-graining simulation method: application on polyethylene." J. Phys. Chem. B **110**: 24093-24100.

Curcó, D. and C. Alemán (2007). "Coarse-grained simulations of amorphous and melted polyethylene." Chem. Phys. Lett. **436**: 189-193.

Dallavalle, M. and N. F. A. van der Vegt (2017). "Evaluation of mapping schemes for systematic coarse graining of higher alkanes." Phys. Chem. Chem. Phys. **19**: 23034-23042.

de Gennes, P.-G. (1971). "Reptation of a polymer chain in the presence of fixed obstacles." J. Chem. Phys. **55**: 572-579.

Doi, M. and S. F. Edwards (1986). The Theory of Polymer dynamics. U.K., Oxford University.

Everaers, R., S. K. Sukumaran, G. S. Grest, C. Svaneborg, A. Sivasubramanian and K. Kremer (2004). "Rheology and microscopic topology of entangled polymeric liquids." Science **303**: 823-826.

Ferry, J. D. (1980). Viscoelastic properties of polymers, John Wiley.

Fetters, L. J., D. J. Lohse, S. T. Milner and W. W. Graessley (1999). "Packing length influence in linear polymer melts on the entanglement, critical, and reptation molecular weights." Macromolecules **32**: 6847-6851.

Fritz, D., K. Koschke, V. A. Harmandaris, N. F. van der Vegt and K. Kremer (2011). "Multiscale modeling of soft matter: scaling of dynamics." Phys. Chem. Chem. Phys. **13**: 10412-10420.

Fukunaga, H., J.-i. Takimoto and M. Doi (2002). "A coarse-graining procedure for flexible polymer chains with bonded and nonbonded interactions." J. Chem. Phys. **116**: 8183-8190.

Graessley, W. and S. Edwards (1981). "Entanglement interactions in polymers and the chain contour concentration." Polymer **22**: 1329-1334.
Grest, G. S. (2016). "Communication: Polymer entanglement dynamics: Role of attractive interactions." J. Chem. Phys. **145**: 141101.
Guerrault, X., B. Rousseau and J. Farago (2004). "Dissipative particle dynamics simulations of polymer melts. I. Building potential of mean force for polyethylene and cis-polybutadiene." J. Chem. Phys. **121**: 6538-6546.
Harmandaris, V. A. and K. Kremer (2009). "Dynamics of Polystyrene Melts through Hierarchical Multiscale Simulations." Macromolecules **42**: 791-802.
Harmandaris, V. A., D. Reith, N. F. A. van der Vegt and K. Kremer (2007). "Comparison between coarse-graining models for polymer systems: two mapping schemes for polystyrene." Macromol. Chem. Phys. **208**: 2109-2120.
Hou, J.-X. (2017). "Note: Determine entanglement length through monomer mean-square displacement." J. Chem. Phys. **146**: 026101.
Hoy, R. S., K. Foteinopoulou and M. Kröger (2009). "Topological analysis of polymeric melts: Chain-length effects and fast-converging estimators for entanglement length." Physical Review E **80**: 031803.
Hoy, R. S. and G. S. Grest (2007). "Entanglements of an end-grafted polymer brush in a polymeric matrix." Macromolecules **40**: 8389-8395.
Hsu, H.-P. and K. Kremer (2016). "Static and dynamic properties of large polymer melts in equilibrium." J. Chem. Phys. **144**: 154907.
Hsu, H.-P. and K. Kremer (2017). "Detailed analysis of Rouse mode and dynamic scattering function of highly entangled polymer melts in equilibrium." Euro. Phys. J. Special Topics **226**: 693-703.
Jorgensen, W. L., J. D. Madura and C. J. Swenson (1984). "Optimized Intermolecular Potential Functions for Liquid Hydrocarbons." J. Am. Chem. Soc. **106**: 6638-6646.
Jorgensen, W. L., D. S. Maxwell and J. Tirado-Rives (1996). "Development and Testing of the OPLS All-Atom Force Field on Conformational Energetics and Properties of Organic Liquids." J. Am. Chem. Soc. **118**(45): 11225-11236.
Karimi-Varzabeh, H. A., N. F. A. van der Vegt, F. Mueller-Plathe and P. Carbone (2012). "How Good are Coarse-Grained Models? A Comparison for Actatic Polystryene." ChemPhysChem **13**: 3428-3439.
Kremer, K. and G. S. Grest (1990). "Dynamics of entangled linear polymer melts: A molecular-dynamics simulation." J. Chem. Phys. **92**: 5057-5086.
Li, Y., B. C. Abberton, M. Kröger and W. K. Liu (2013). "Challenges in Multiscale Modeling of Polymer Dynamics." Polymers **5**: 751-832.
Likhtman, A. E. and T. C. McLeish (2002). "Quantitative theory for linear dynamics of linear entangled polymers." Macromolecules **35**: 6332-6343.
Lodge, T. P. (1999). "Reconciliation of the molecular weight dependence of diffusion and viscosity in entangled polymers." Physical Review Letters **83**: 3218.
Marrucci, G. (1985). "Relaxation by reptation and tube enlargement: A model for polydisperse polymers." J, Polym. Sci. Part B: Polym. Phys. **23**: 159-177.
Martin, M. G. and J. I. Siepmann (1998). "Transferable potentials for phase equilibria. 1. United-atom description of n-alkanes." J. Phys. Chem. B **102**: 2569-2577.
Maurel, G., F. Goujon, B. Schnell and P. Malfreyt (2015). "Prediction of structural and thermomechanical properties of polymers from multiscale simulations." RSC Advances **5**(19): 14065-14073.
Maurel, G., B. Schnell, F. Goujon, M. Couty and P. Malfreyt (2012). "Multiscale modeling approach toward the prediction of viscoelastic properties of polymers." Journal of Chemical Theory and Computation **8**: 4570-4579.
Milano, G. and F. Müller-Plathe (2005). "Mapping atomistic simulations to mesoscopic models: A systematic coarse-graining procedure for vinyl polymer chains." J. Phys. Chem. B **109**: 18609-18619.

Müller-Plathe, F. (2002). "Coarse-graining in polymer simulation: from the atomistic to the mesoscopic scale and back." ChemPhysChem **3**: 754-769.
Nath, S. K., F. A. Escobedo and J. J. de Pablo (1998). "On the simulation of vapor–liquid equilibria for alkanes." J. Chem. Phys. **108**: 9905-9911.
Padding, J. and W. J. Briels (2001). "Uncrossability constraints in mesoscopic polymer melt simulations: non-Rouse behavior of C 120 H 242." J. Chem. Phys. **115**: 2846-2859.
Padding, J. and W. J. Briels (2002). "Time and length scales of polymer melts studied by coarse-grained molecular dynamics simulations." J. Chem. Phys. **117**: 925-943.
Padding, J. and W. J. Briels (2011). "Systematic coarse-graining of the dynamics of entangled polymer melts: the road from chemistry to rheology." J. Phys. Cond. Matter **23**: 233101.
Paul, W., D. Y. Yoon and G. D. Smith (1995). "An optimized united atom model for simulations of polymethylene melts." J. Chem. Phys. **103**: 1702-1709.
Peter, C. and K. Kremer (2009). "Multiscale simulation of soft matter systems – from the atomistic to the coarse-grained level and back." Soft Matter **5**: 4357–4366.
Peters, B. L., K. M. Salerno, A. Agrawal, D. Perahia and G. S. Grest (2017). "Coarse Grained Modeling of Polyethylene Melts: Effect on Dynamics." J. Chem. Theory Comp. **13**: 2890-2896.
Peters, B. L., K. M. Salerno, T. Ge, D. Perahia and G. S. Grest (2018). "Dynamics of Polydispersed, Entangled Polymer Melts." in preparation.
Plimpton, S. (1995). "Fast parallel algorithms for short-range molecular dynamics." J. Comp. Phys. **117**: 1-19.
Reith, D., M. Pütz and F. Müller-Plathe (2003). "Deriving effective mesoscale potentials from atomistic simulations." Journal of computational chemistry **24**: 1624-1636.
Richter, D., R. Butera, L. Fetters, J. Huang, B. Farago and B. Ewen (1992). "Entanglement constraints in polymer melts. A neutron spin echo study." Macromolecules **25**: 6156-6164.
Salerno, K. M., A. Agrawal, D. Perahia and G. S. Grest (2016). "Resolving Dynamic Properties of Polymers through Coarse-Grained Computational Studies." Phys. Rev. Lett. **116**: 058302.
Salerno, K. M., A. Agrawal, B. L. Peters, D. Perahia and G. S. Grest (2016). "Dynamics in entangled polyethylene melts." Euro. Phys. J. Special Topics **225**: 1707-1722.
Salerno, K. M. and N. Bernstein (2018). "Persistence Length, End-End Distance and Structure of Coarse-Grained Polymers." J. Chem. Theory Comp. **14**: 2219–2229.
Schleger, P., B. Farago, C. Lartigue, A. Kollmar and D. Richter (1998). "Clear evidence of reptation in polyethylene from neutron spin-echo spectroscopy." Phys. Rev. Lett. **81**: 124-127.
Siepmann, J. I., S. Karaborni and B. Smit (1993). "Simulating the critical properties of complex fluids." Nature **365**: 330-332.
Sirk, T. W., Y. R. Slizoberg, J. K. Brennan, M. Lisal and J. W. Andzelm (2012). "An enhanced entangled polymer model for dissipative particle dynamics." J. Chem. Phys. **136**: 134903.
Siu, S. W., K. Pluhackova and R. A. Böckmann (2012). "Optimization of the OPLS-AA force field for long hydrocarbons." J. Chem. Theory Comp. **8**: 1459-1470.
Sun, Q. and R. Faller (2005). "Systematic coarse-graining of atomistic models for simulation of polymeric systems." Computers Chem, Eng, **29**: 2380-2385.
Vega, J. F., S. Rastogi, G. W. M. Peters and H. E. H. Meijer (2004). "Rheology and reptation of linear polymers. Ultrahigh molecular weight chain dynamics in the melt." J. Rheology **48**: 663-678.
Voth, G. A. (2008). Coarse-graining of condensed phase and biomolecular systems, CRC press.
Wang, H., C. Junghans and K. Kremer (2009). "Comparative atomistic and coarse-grained study of water: What do we lose by coarse-graining?" Euro. Phys. J. E **28**: 221-229.

Figures

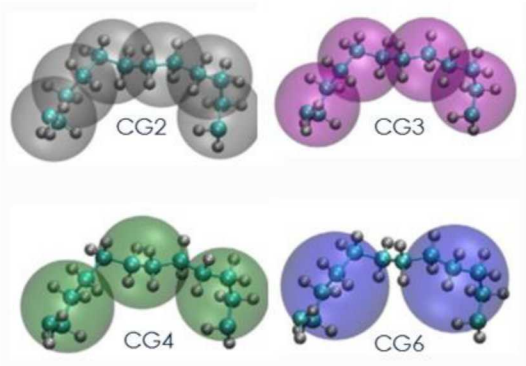

Figure 1. $C_{12}H_{24}$ segment of a PE chain represented with degree of coarse graining λ=2, 3, 4, and 6 methylene groups per CG bead. The bead diameter corresponds to the position of the minimum in the nonbonded interaction for each CG model.

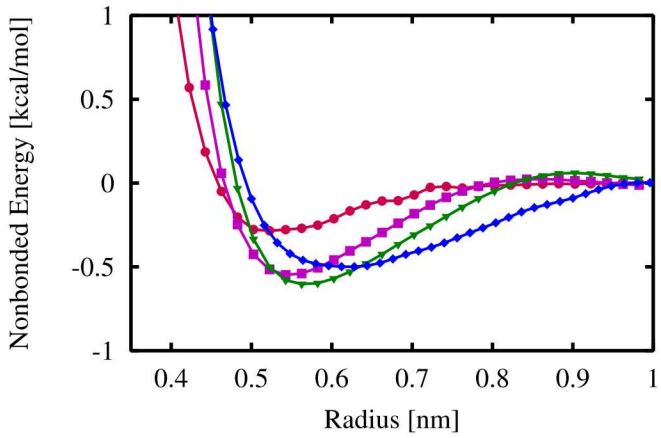

Figure 2. Potentials for nonbonded interactions for λ = 2 (red circle), 3 (purple square), 4 (green triangle and 6 (blue diamond).

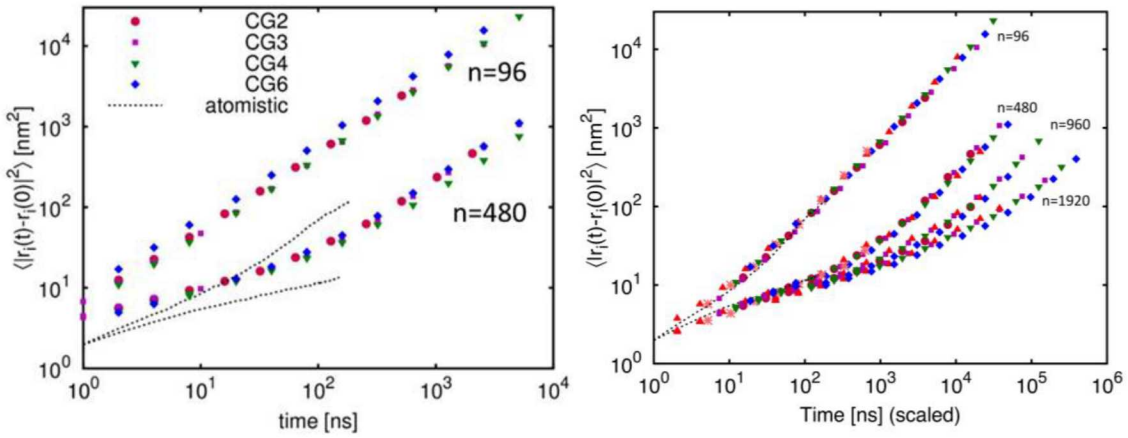

Figure. 3. (a) Mean squared displacement of the inner 24 -CH_2- groups of each polymer chain at 500 K for different levels of coarse graining compared to atomistic model for n = 96 and 480. (b) Coarse grained MSD data scaled by dynamic rescaling factor α for n = 96 – 1920 compared to atomistic simulations.

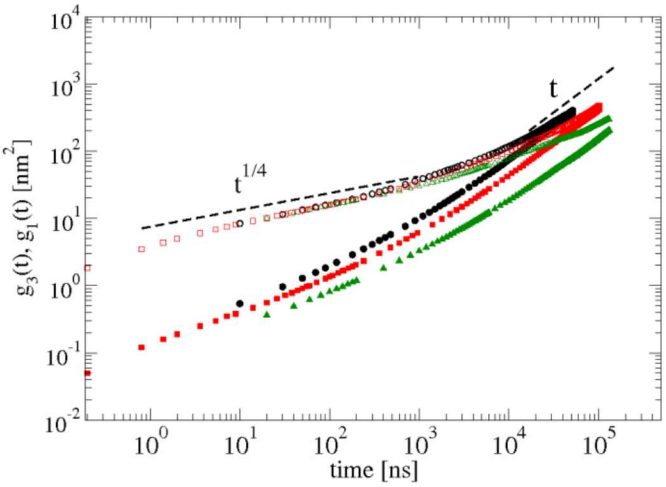

Figure 4. Mean squared displacement of the center of mass $g_3(t)$ (closed) and center four CG beads $g_1(t)$ (open) for n = 1920 (black circles), 2560 (red squares) and 4000 (green triangles) for λ = 4. The dashed lines represent the scaling predictions t^1 for the diffusive regime and $t^{1/4}$ for the reptation regime.

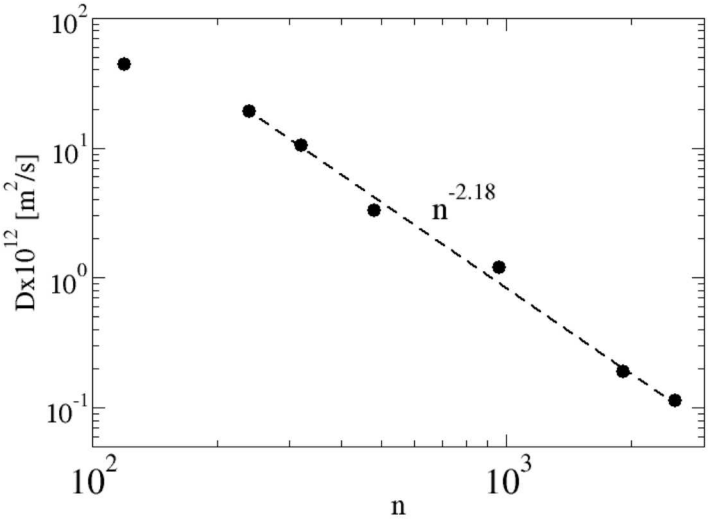

Figure 5. Diffusion constant D versus n for λ =4 at 500 K.

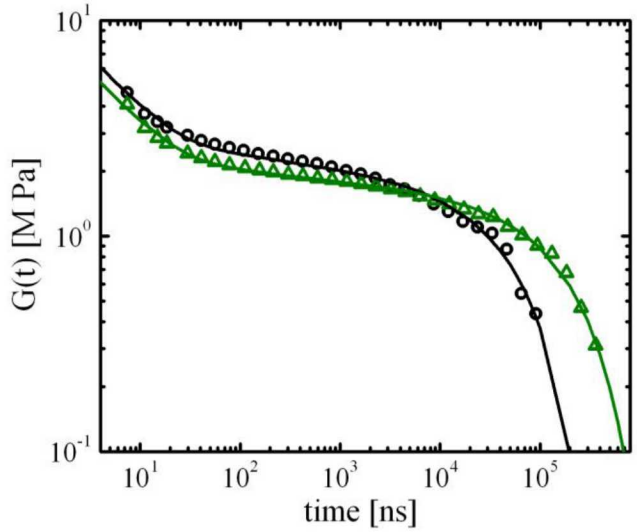

Figure 6. Stress autocorrelation function G(t) for λ = 4 at 500 K for n = 1920 (black) and 4000 (greeen). Solid lines are fit to the Likhtman-McLeish formula (Likhtman and McLeish 2002).

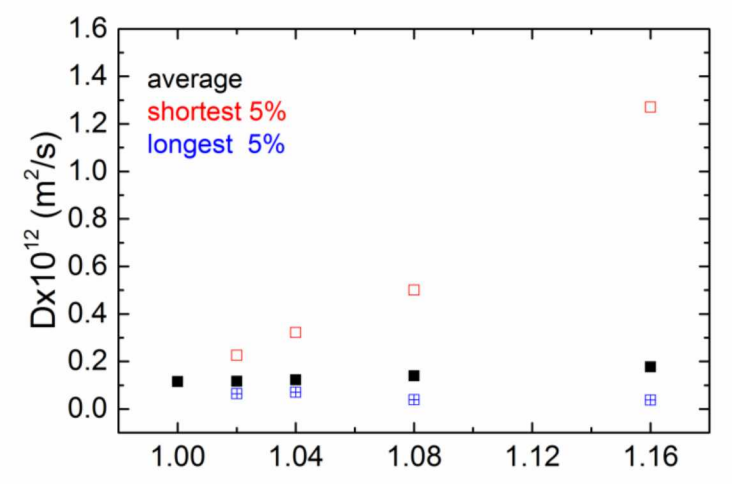

Figure 7. Diffusion constant D as a function of molar-mass dispersity $Đ_M$ averaged over all the chains (black), for the shortest 5% of the chains (red), and longest 5% of the chains (blue) for n = 2560 for λ = 4.5